

# Insulating Piles for the Cost-effective Construction of Very Large-scale High Temperature Thermal Energy Storage

Alice Tosatto<sup>1,\*</sup>, Fabian Ochs<sup>1</sup>, Abdulrahman Dahash<sup>1,2</sup>, Christoph Muser<sup>3</sup>, Felix Kutscha-Lissberg<sup>4</sup>, Peter Kremnitzer<sup>4</sup>

<sup>1</sup> Unit of Energy Efficient Building, University of Innsbruck, Innsbruck, Austria

<sup>2</sup> Sustainable Thermal Energy Systems, Center for Energy, AIT Austrian Institute of Technology GmbH, Vienna, Austria

<sup>3</sup> ste.p ZT-GmbH, Vienna, Austria

<sup>4</sup> PORR Bau GmbH, Vienna, Austria

\*Email: [alice.tosatto@uibk.ac.at](mailto:alice.tosatto@uibk.ac.at)

**Abstract**—Large-scale thermal energy storage (TES) represents a key component in renewables-based district heating (DH) networks. However, the storage of water at high temperature (< 100 °C) for long periods can lead to a significant amount of thermal losses to the surroundings and to unwanted increase of groundwater temperature. Insulating the side walls is consequently required, but it is associated with large investment costs. Installation represents a high share of the total investment costs of the insulation, which has to be temperature and pressure resistant and resistant against humid environments. Hence, costs-effective insulation installation methods and processes supported by a proper envelope design are crucial.

The new approach proposed in this work is based on the use of overlapping bore piles and considers the use of piles filled with foam glass gravel (FGG) as insulation. The advantages of this solution rely on the possibility to reduce the installation costs and on the thermal characteristics of the adopted material. FGG is a frequently used insulation material in underground constructions due to its low thermal conductivity, pressure resistance and draining properties and relatively low cost. FGG can be used with a loose, compacted or bounded configuration. While the loose material outperforms the bounded in terms of thermal conductivity, the second one presents improved structural properties. One approach is to alternate bounded and loose piles where the bounded represent the primary piles and these are overdrilled producing the loosely filled secondary piles. An alternative is to use different degree of compaction in the primary and secondary piles. A compromise between required strength and thermal performance has to be found. The paper reports results of material tests, mock-ups and simulation results.

**Keywords:** Thermal Energy Storage, Insulation, Foam glass gravel, Thermal conductivity, Natural convection, Material testing.

## 1. INTRODUCTION

The concept of large-scale thermal energy storage (TES) in renewables-based district heating (DH) systems was first employed in Sweden in 1985, while in the last years in Denmark this technology has been improved and extensively used [1]. The term “Danish pit” refers therefore to a specific construction type of TES, whose characteristics are a truncated pyramid shape, an insulated floating cover, the absence of thermal insulation on the side and bottom walls and the use of a welded impermeable polymeric liner to prevent water losses and infiltration, as in the systems present in Marstal, Dronninglund and Gram [2][3]. The exploitation of this technology in other locations (e.g. urban environment) with different ground conditions (e.g. presence of groundwater) requires, however, the development of alternative construction methods (e.g. improved storage compactness, low environmental impact). In particular, thermal insulation is one of the most important components in order to deal with predefined regulations with regard to groundwater protection. This work will therefore focus on the study of the possible insulation solutions and on a new insulation design concept, the foam glass gravel (FGG) insulating bore piles.

This study is carried out by means of numerical simulations and material tests. In particular, numerical simulations were used to evaluate the effectiveness of insulating bore piles with different FGG characteristics and different interval distances. Then a downscaled pre-mock-up of a pile filled with FGG was realised at the Unit of Energy Efficient Buildings of the University of Innsbruck, in order to

test the measurement set-up in view of future field-tests and investigate the thermal behaviour of the insulating material.

## **2. CONSTRUCTION OF BURIED LARGE-SCALE TES**

A truncated cone for thermal storage purpose, although easy to apply in terms of excavation work, is not the ideal solution when looking at the actual storage efficiency. The large cover surface represents the weakest element of the envelope because of its direct contact with the external air and results in significant thermal losses leading to a poor thermal stratification [4].

With these considerations, a cylindrical TES shape (buried tank TES) is a promising alternative [5]: a favourable height-to-diameter ratio (also known as aspect ratio AR) results in lower thermal losses from the cover, whereas the surrounding ground acts as a thermal damper thanks to its thermal capacity. Moreover, a more compact structure allows saving land space, resulting in lower land costs and an increased social acceptance.

However, the construction of vertical walls represents a big challenge in the structural stability of the storage. The diaphragm wall (see Figure 1) in this case is the most indicated solution, but in case of larger TES diameter, it requires a proper support (i.e. retaining ground anchors) to stop eventual sliding movements (e.g. buckling).

The presence of groundwater is another important aspect that needs to be considered. In Danish pits, the excavated soil is used to build embankment walls around the storage, thus preventing the overall structure to reach the depth of the groundwater table. This solution may not be always acceptable (e.g. visual impact) or sufficient (e.g. shallow groundwater

table). The use of a cut-off wall, which is a vertical barrier with low water permeability, is a good strategy to minimize the groundwater flow around the TES [6]. Moreover, thermal insulation is a key to prevent the groundwater overheating. Considering the high costs required to insulate a buried tank TES, an effective insulation may not be economically feasible, but it is necessary to face the aforementioned problems [7]. A reduction of material and installation costs is therefore desirable for the feasibility of this promising technology. Location, thickness and material of the insulation have to be technically defined in the planning phase of the TES, since they can significantly contribute to the costs. This work will focus on the technical aspects, concerning insulation material, design and location.

## **3. THERMAL INSULATION IN LARGE-SCALE TES**

In case of pit TES, typically only the cover is insulated (an exception is the Eggenstein-Leopoldshafen TES). In buried tank TES the insulation can be placed either inside or outside the static structure. The insulation was installed outside the concrete structure in Rottweil, Friedrichshafen and Munich, while in the gravel water TES in Chemnitz it was inside the sheet pile wall [8].

The ideal location of insulation is close to the element to be insulated (i.e. water domain), in order to minimize the energy dissipation towards the surroundings. The internal-insulation solution shows, however, some disadvantages linked to the performance of the insulating material itself. The high temperatures of the storage (up to 90-95 °C according to the supply temperature of the local DH) and the water infiltrations can contribute to a rapid degradation of the insulation materials [9]. Moreover, a frequent change of insulation is not feasible in terms of costs and optimal TES operation.



**Figure. 1** Diaphragm wall construction and shaft with diaphragm walls (photos courtesy of PORR).

The operation characteristics of the TES (i.e. temperature range) and the ground conditions (i.e. soil thermal conductivity, presence of groundwater) as well as the location within the envelope itself (i.e. cover, sidewalls, base) are important parameters to consider in the selection of the insulation material. Some of the most suitable materials used for the insulation of large-scale TES systems are listed in Table 1 [8] [10] [11]. The optimal distribution and design of the insulation as component is a factor worthy of attention, since it contributes for a significant part to the efficient operation of a buried TES.

**4. CONCEPT OF INSULATING PILE**

**Table 1.** Insulation materials for buried TES systems: thermal conductivity ( $\lambda$ ) and specific cost.

Insulation material	$\lambda$ [W/(m·K)]	Cost [€/m <sup>3</sup> ]	Ref.
Polyurethane (PUR)	0.025-0.03	160-200	[10] [11]
Expanded polystyrol (EPS)	0.030-0.044	60-130	[10] [11]
Extruded polystyrol (XPS)	0.035-0.042	100-160	[10] [11]
Perlite	0.05-0.06		[8]
Expanded Clay (EC)	0.08-0.1		[8]
Expanded Glass Granules (EGG)	0.07-0.08		[8]
Glass Wool	0.035-0.044	110-130	[10] [11]
Foam Glass (CG)	0.05-0.06		[10]
Foam Glass Gravel (FGG)	0.08-0.15	70-100	[10] [11]

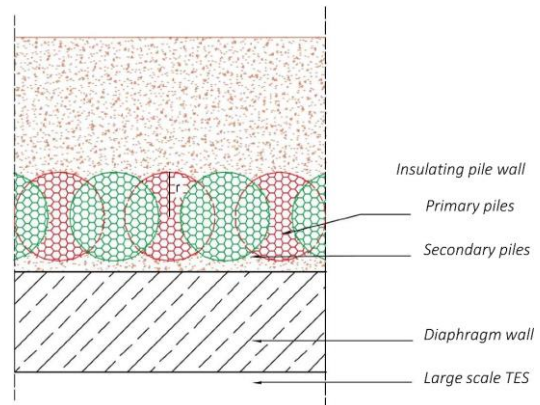
**WALL**

Besides the cost of the material itself, the installation of thermal insulation is another cost item affecting the planning of the TES. The concept developed by the consortium of the “giga\_TES” project [12] consists in the construction of an insulating bore pile wall that can be drilled around the storage. This solution represents a step forward from the current use of concrete piles, already quite

common in geotechnics for the construction of shafts (see Figure 2).



(a)



(b)

**Figure 2.** (a) Top view of a shaft with concrete piles (photo courtesy of PORR) and (b) horizontal section of a schematic representation of a TES envelope with insulating bore piles.

For the specific application under study, the first requirement of the insulation material is that it can be poured from above without the need for scaffolding. Bulk materials like perlite, expanded clay (EC) and foam glass gravel (FGG) are suitable for this application, but only FGG presents a sufficient stability thanks to its friction angle (“*Schüttwinkel*”) of almost 40° [13] to allow subsequent over-drillings to create a wall of bore piles. The second requirement is the material’s good resistance to pressure and high temperatures (the TES would be at 90 °C under full load conditions) and its durability in a humid environment like the soil. This second requirement shortens the list of available materials by eliminating insulation like PUR and EPS. Then, a competitive cost per unit volume is the third selection criterion

considering the large quantity of material required; however, to consider it alone would be misleading, as it should be combined with the installation costs.

The goal of this study is the development of new insulation installation solutions that can compete with the currently available strategies. FGG represents in this perspective a valid material choice already extensively used in seasonal TES systems (e.g. Munich and Eggenstein-Leopoldshafen [14]), since it is pressure resistant, lightweight, environmentally sustainable, resistant to ageing and to acid- or alkali-environments and easily shapeable [8] [13]. However, the granular structure of this material must also be considered, since it may lead to increased thermal flux due to convection and radiation [14] [15].

The design concept of the insulating bore pile wall is shown in Figure 2b. It consists of a sequence of primary (I) and secondary (II) drilled piles, filled with FGG. Primary piles can be composed of bounded or loose FGG, the secondary piles are instead made of loose FGG.

The optimal combination of bounded and loose material considers the structural stability of the pile and its insulation performance (i.e. ability to maintain ground temperatures within the limits). The purpose of this work is thereby to provide some indication on the insulating performance of the FGG under different material configurations, in order to evaluate the influence of the different heat transfer phenomena.

## 5. NUMERICAL SIMULATIONS

Finite elements (FE)-based numerical simulations are a powerful mean to investigate a wide variety of geometries and materials combinations with minimal cost and time consumption. The presented results were obtained using COMSOL Multiphysics 5.4. This first part of the study was carried out in an early phase to guide the following mock-ups' test phase. In particular, the effectiveness of the use of bounded FGG for primary piles was investigated and compared with the use of loose FGG only.

The simulations investigated the behaviour of the different FGG configurations (loose or bounded) and

the geometrical distribution of the piles (i.e. distance  $d$  between the piles). The material properties used as inputs are presented in Table 2. Bounded FGG consists in a cohesive structure of FGG granules, which presents a poorer insulating performance compared to the traditional loose FGG, since the cement-based material used to maintain the grains' cohesion has a higher thermal conductivity.

A simplified TES temperature profile was defined to simulate its seasonal operation: in summer the storage is filled with water at 90 °C, while in winter water at 60 °C is injected in the storage to substitute the amount extracted to supply the DH network. Standard ground conditions were considered, i.e. absence of groundwater and constant thermal properties.

For the sake of simplicity, only conductive heat transfer in the envelope and the surrounding ground was considered, as from Equation (1)

$$\dot{q} = \lambda \frac{\Delta T}{\Delta x} \quad (1)$$

where  $\lambda$  is the nominal thermal conductivity of the material. In particular, the terminology for the thermal conductivity used in the following paragraphs is  $\lambda_I$ , for the primary piles, and  $\lambda_{II}$ , for the secondary piles (assumed always filled with loose material, so that  $\lambda_{II}=0.08$  W/(m·K)).

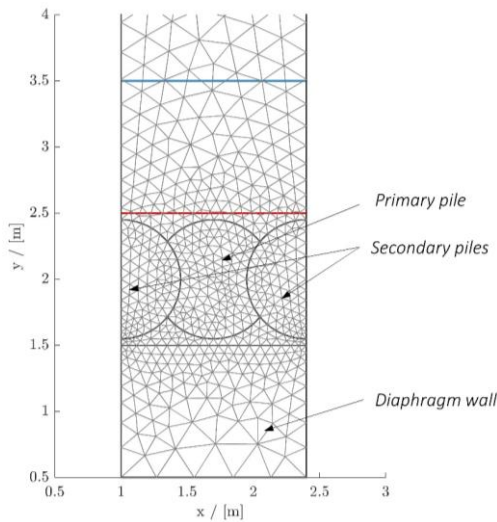
**Table 2.** Input material properties: thermal conductivity  $\lambda$ , density  $\rho$  and specific heat at constant pressure  $c_p$ .

	$\lambda$ [W/(m·K)]	$\rho$ [kg/ m <sup>3</sup> ]	$c_p$ [J/ (kg·K)]	Ref.
FGG loose uncompacted	0.08	150	750	[10]
FGG bounded	[0.2 ... 0.4]	[600 ... 1000]	1000	own measurements
Concrete	2.5	2300	1000	[10]
Ground	[1.5 2.5]	1000	880	[10]

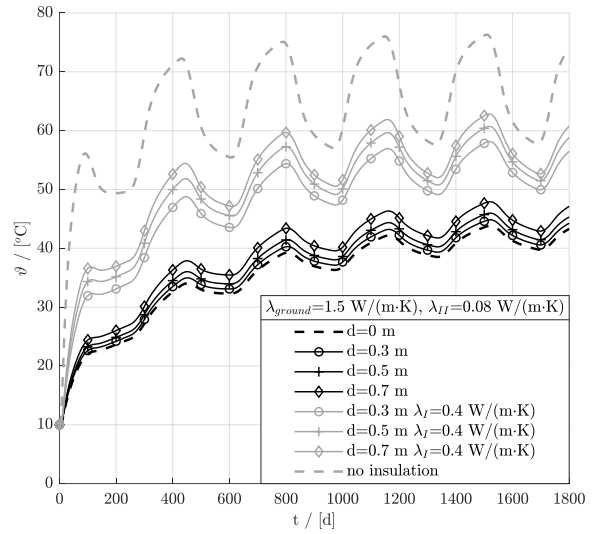
The initial ambient (i.e. ground) temperature is set to 10 °C. A total simulation period of 5 years (assuming for simplicity a year of 360 days with time interval of 1 day) was used for the analysis. The geometry implemented for the study is presented in Figure 3. Thermal losses and maximum ground temperature were evaluated respectively on the red and blue lines in Figure 3.

Figure 4 presents the simulation results for the different configurations in the cases of ground thermal conductivity of 1.5 W/(m·K) and 2.5 W/(m·K). Lower ground thermal conductivities appear to ensure higher temperatures in the ground. A low ground thermal conductivity determines a lower dissipation of the thermal energy stored, thus maintaining higher temperatures in the region close to the TES.

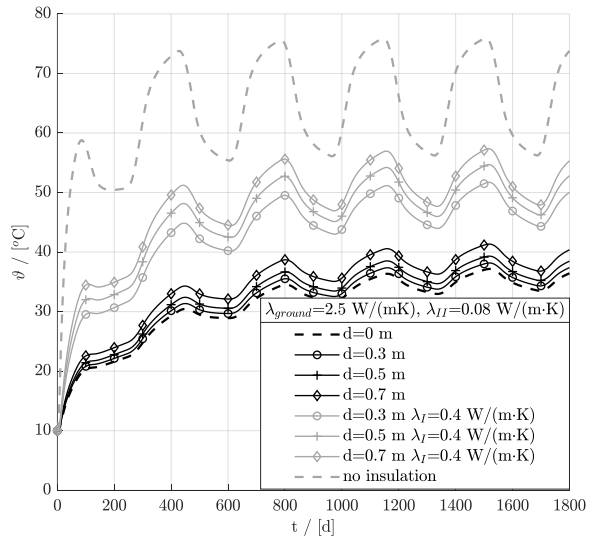
In the case with ground thermal conductivity of 1.5 W/(m·K) (Figure 4a), we observe that under the simulated boundary conditions the use of bounded primary piles (continuous grey lines) can reduce the ground temperatures at 1 m distance from the borehole envelope down to 18 K, compared to the case without insulation. Instead, the use of loose material only (continuous black lines) ensures a reduction of about 28 K.



**Figure 3.** Geometry, mesh and location of the probes for ground temperature evaluation (blue line) and thermal losses integration (red line).



(a)

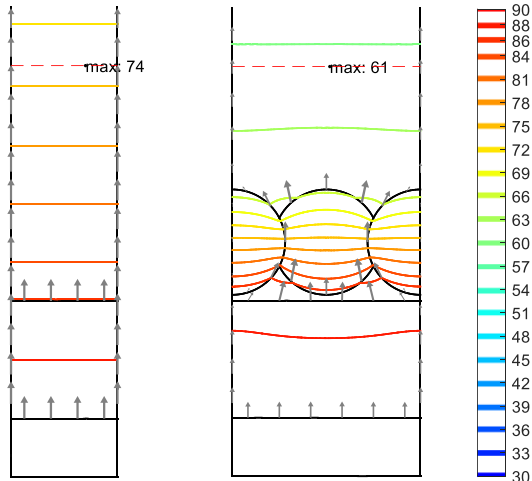


(b)

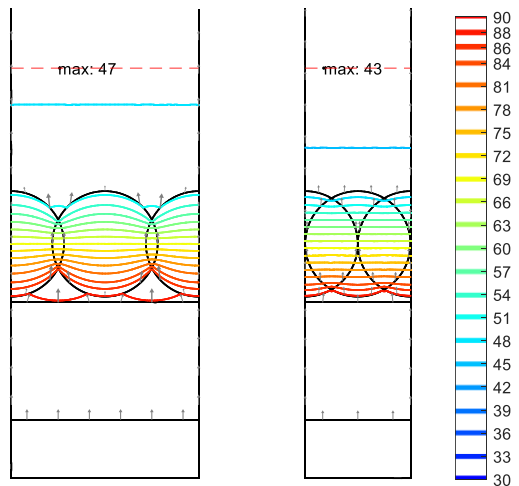
**Figure 4.** Ground temperature profiles for ground thermal conductivity of (a) 1.5 W/(m·K) and (b) 2.5 W/(m·K). The dashed lines show the limit cases of no insulation (in grey) and distance  $d=0 \text{ m}$  between the secondary piles with no use of bounded material ( $\lambda_I=\lambda_{II}$ ) (in black). The continuous black lines present the cases with no use of bounded material ( $\lambda_I=\lambda_{II}$ ) and different distances between the secondary piles, whereas the continuous grey lines present the cases with bounded primary piles ( $\lambda_I=0.4 \text{ W/(m}\cdot\text{K)}$ ) and loose secondary piles ( $\lambda_{II}=0.08 \text{ W/(m}\cdot\text{K)}$ ).

A more detailed presentation of the influence of the bore pile structure on the ground temperature is provided in Figure 5, which shows for some of the examined structures the isothermal curves at the end of the simulated period, when the TES is full at 90 °C.

In the case with bounded primary piles (Figure 5a), the heat flux concentrates in the sections with minor thermal resistance, thus reducing the insulating effect of the loose secondary piles. Homogeneous



(a)



(b)

**Figure 5.** Isothermal curves in the TES envelope and surrounding ground ( $\lambda_{ground}=1.5 \text{ W}/(\text{m}\cdot\text{K})$ ) at the end of the simulation period (temperatures are in [°C]). (a) Insufficient insulation performance in the case of no insulation and in the case of bounded primary piles ( $\lambda_I=0.4 \text{ W}/(\text{m}\cdot\text{K})$ ) with distance  $d=0.7 \text{ m}$  between the secondary piles. (b) Examples of effective insulation in the cases of  $d=0.7 \text{ m}$  and  $d=0 \text{ m}$  with loose primary piles.

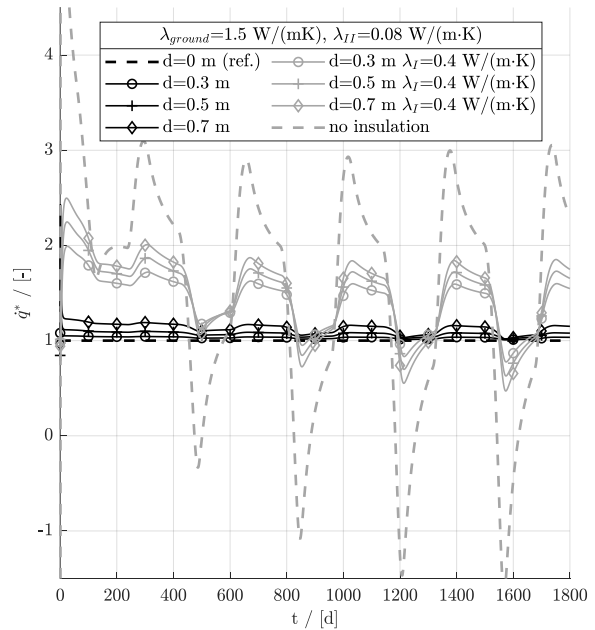
thermal properties are recommended to avoid the formation of zones with different thermal resistance than can enhance the local heat transfer (Figure 5b).

Figure 6 presents the specific thermal losses relative to the reference case (as from Equation (2)), which is set to be the configuration with  $d=0 \text{ m}$  and loose material only (i.e. same material configuration for primary and secondary piles,  $\lambda_I=\lambda_{II}$ ).

$$q^* = \frac{\dot{q}_i}{\dot{q}_{ref}} \quad (2)$$

While the use of loose FGG for the primary piles (continuous black lines) guarantees minimal additional thermal losses even increasing the distance between the piles, the use of bounded FGG (continuous grey lines) leads to significantly higher losses during the charging and storage phases, but lower during the discharging phase. This is again explained by the storage effect of the ground: the higher thermal losses observed when the TES is full at 90 °C result in an increased heating of the surrounding ground, which acts as a thermal damper. This phenomenon is even more evident in the case of no insulation (grey dashed line).

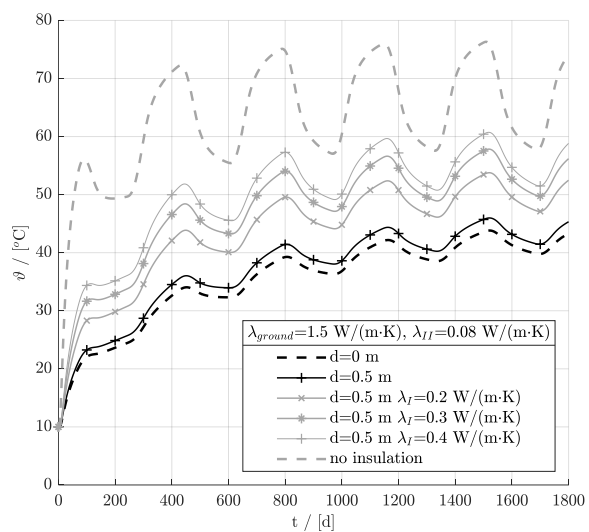
Overall, the use of insulation provides a remarkable reduction of the ground temperature. However, it is clear from this preliminary study, that the use of bounded FGG (in the primary piles) with a thermal conductivity significantly higher than the



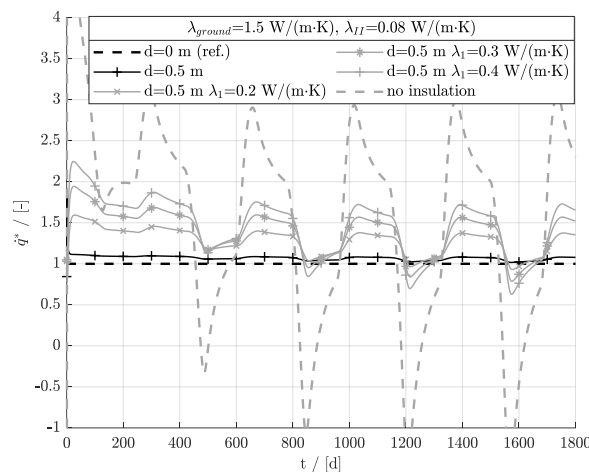
**Figure 6.** Specific thermal losses related to the best case (with  $d=0 \text{ m}$  and  $\lambda_I=\lambda_{II}$ ) for the configurations and the ground conductivity presented in Figure 4a.

thermal conductivity of the loose FGG used in the secondary piles nullifies the insulating performance of the latter.

The graphs in Figure 7 present the ground temperature and the specific thermal losses for different primary piles configurations. It appears that (for the same distance between the secondary piles) the use of bounded material with lower thermal conductivity (i.e.  $\lambda_f=0.2$  W/(m·K) instead of  $\lambda_f=0.4$  W/(m·K)) ensures lower ground temperatures and lower thermal losses. However, even this configuration is outperformed by the use of loose material only (as can be seen from the annual losses in Table 3).



(a)



(b)

**Figure 7.** (a) Ground temperature profiles in the cases of ground thermal conductivity of 1.5 W/(m·K) and different thermal performance ( $\lambda_f$ ) of bounded FGG and (b) relative specific thermal losses related to the best case.

With these considerations, it is advisable the use of loose FGG (possibly compacted to guarantee more stability) to substitute the bounded FGG in primary piles. Further experimental investigations regarding the insulating performance and the stability of the compacted FGG are then carried out.

**Table 3.** Cumulative annual thermal losses for different typologies of FGG employed in primary piles, compared to the best case, for the 5<sup>th</sup> year of operation.

Case	$\Delta q$
$d=0$ m, $\lambda_f=\lambda_{f1}=0.08$ W/(m·K) – best case	(reference)
$d=0.5$ m, $\lambda_f=\lambda_{f1}=0.08$ W/(m·K)	+6%
$d=0.5$ m, $\lambda_f=0.2$ W/(m·K)	+25%
$d=0.5$ m, $\lambda_f=0.3$ W/(m·K)	+35%
$d=0.5$ m, $\lambda_f=0.4$ W/(m·K)	+42%

## 6. INSULATING PILE PRE-MOCK-UP TESTS

With the purpose of better studying the thermal behaviour of the material and testing the experimental set-up for further field tests, a downscaled pre-mock-up of a FGG pile was realised. In particular, considering the outputs of the simulations analysis, where the loose FGG appeared to outperform the bounded FGG, this test investigated the heat transport in the loose material under different configurations (e.g. uncompacted and compacted). The planned following field tests consist in realising real scale bore pile mock-ups, in order to test the structural stability of the compacted material and its applicability in the primary piles. Moreover, the actual performance of the material with boundary conditions similar to the ones of a buried tank TES will be tested. The costs associated with piles installation and compaction will be investigated within the next field test phase.

The realised downscaled pre-mock-up was a vertical cylinder of 1 m height and 0.5 m diameter filled with FGG. The measuring probe, hosting the heating device (a 1 m long heating band) and the measuring sensors (Pt100), was located vertically along the symmetry axis of the cylinder. This probe was realized using a stainless steel pipe (35 mm diameter): three Pt100s were attached to the heating device at 250 mm, 500 mm and 750 mm height. The remaining voids in the probe were then filled using quartz sand.

Several material configurations (listed in Table 4) were tested to provide an extensive overview of the possible solutions applicable in the insulation of a buried TES.

**Table 4.** Pre-Mock-up configurations.

Material	$\rho$ [kg/m <sup>3</sup> ]
Loose FGG 10/60 (uncompacted)	150
Loose FGG 10/60 (compacted)	190
Red FGG	205
Loose FGG 10/30	144
Loose FGG mix (50% 10/30 + 50% 10/60)	147

The test consisted in a first phase, when the heating device was heated for 8-10 hours to 90 °C (to simulate the TES temperature), and in a following cooling phase. The temperatures measured by the three Pt100 were collected for the entire test period. The resulting temperature curves measured by the mid Pt100 (at 500 mm height) are presented in Figure 8.

A numerical FE-based model was realized using COMSOL Multiphysics 5.4, in order to evaluate the effective thermal conductivity of the insulating material. To account for the eventual additional convective heat transfer between the FGG grains,

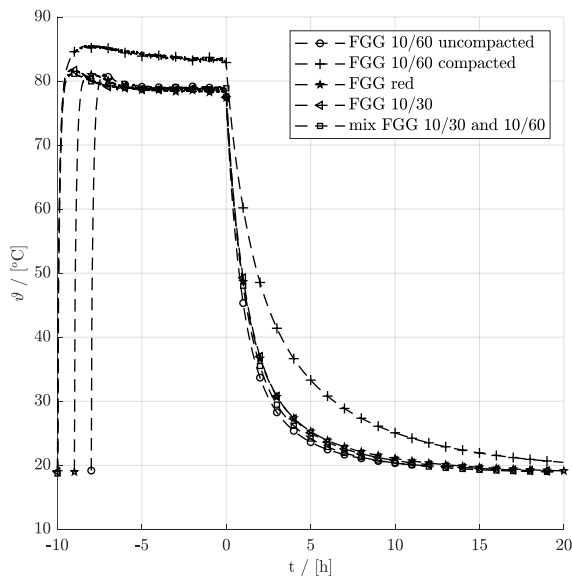


**Figure 8.** Mid sensor measured temperature values (minute average) for the analysed configurations. To better compare the profiles of the cooling curves, the cooling phase is here assumed to start at the time t=0 h.

instead of Equation (1), Equation (3) is used:

$$\dot{q} = h \Delta T \tag{3}$$

where  $h$  represents the convective heat transfer coefficient, which considers the combined effects of conduction and convection expressed through the Nusselt number ( $Nu$ ) that represents the ratio of convection to pure conduction [17] as from Equation (4):

$$h = \frac{Nu \lambda}{\Delta x} \tag{4}$$

The investigation of the role played by natural convection in this application is important to evaluate the actual performance of the material, considering the high temperature gradients involved (i.e. 90 °C of the TES compared to the ground temperatures) and the heat flux direction (i.e. 3D heat flux distribution in the envelope and soil).

The boundary conditions used in the numerical model were the surrounding ambient conditions of the climate chamber where the pre-mock-up was installed. The measured electric power required to keep the mock-up at a temperature of 90 °C for a period of 8 to 10 hours was used as input in the numerical model.

As in the actual measurements, the simulation analysis consisted of an initial heating phase (of 8 to 10 hours) and in a following cooling phase. The resulting temperature profile obtained in the centre of the cylinder was compared with the temperature measured by the middle sensor. The FGG thermal conductivity including the influence of convection ( $\lambda \cdot Nu$ ), which was used as input in the model, was then tuned to fit the measured values: the best fitting value was defined as the effective thermal conductivity of the material. Figure 9 shows the interpolation between the measured and simulated temperature curves under different effective thermal conductivity values for the first investigated configuration (FGG 10/60 uncompacted).

A direct indicator of the insulation performance was the actual electric power required to keep the heating probe at a temperature of 90 °C: lower thermal losses result in a lower required power once the steady state phase is reached (Figure 10).

The effective thermal conductivities resulting from the tests, including the influence of natural convection (expressed by  $\lambda \cdot Nu$ ), are presented in Figure 11.

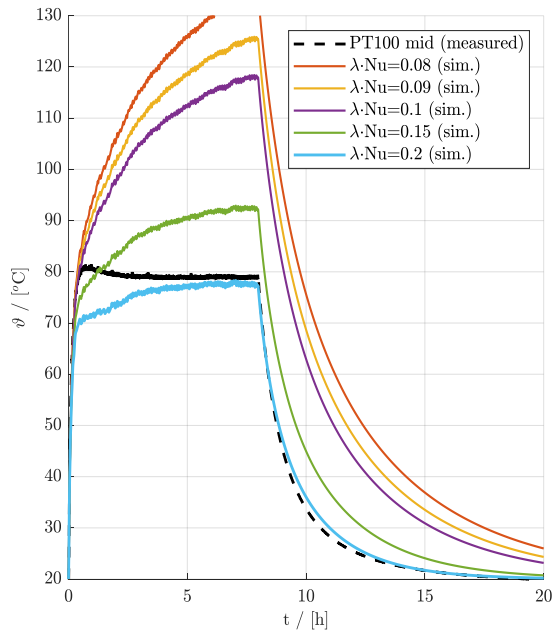


**Figure 9.** Comparison of the measured (dashed lines) and simulated (continuous line) temperatures for the FG configuration “10/60 uncompact”; values of  $(\lambda \cdot Nu)$  are in  $[W/(m \cdot K)]$ .

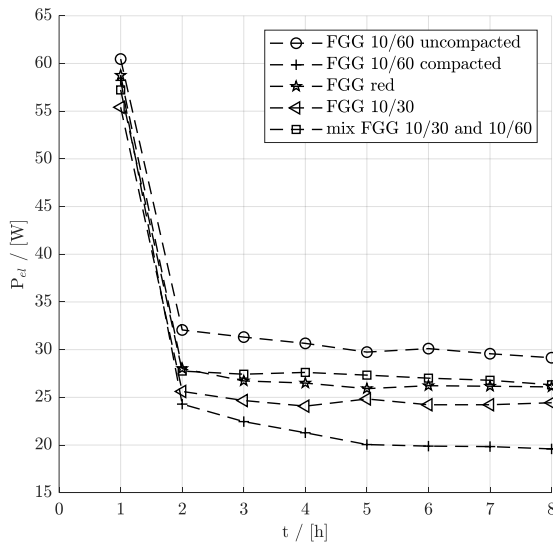


**Figure 10.** Hourly average of the input electric power required during the tests.

## 7. RESULTS AND DISCUSSION

From the pre-mock-up tests, it emerged that the uncompact FGG 10/60 in this application conditions (lateral insulation of a heat source) has a poor insulation performance, compared with the

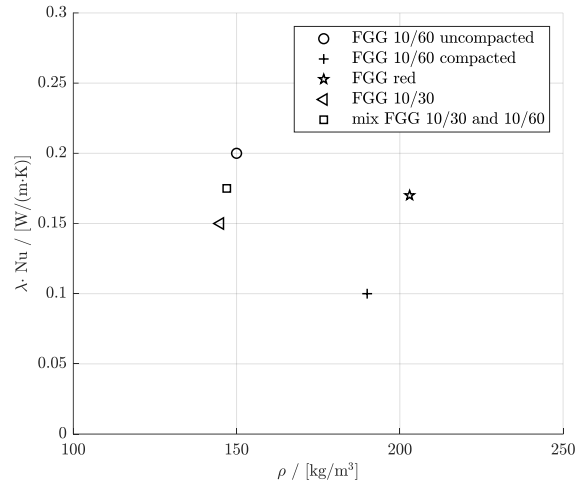


**Figure 11.** Effective thermal conductivity resulting from the pre-mock-up tests, including the natural convection.

compact FGG 10/60 or with the FGG with smaller grain sizes.

As summarised in Figure 11, the compacted material guarantees the best performance in the experimental set-up thanks to the minimisation of the natural convection. The high temperatures involved determine a buoyancy flow within the FGG bulk that enhances the heat transport [15]. The convective heat transfer between the grains therefore increases the effective thermal conductivity of the bulk  $(\lambda \cdot Nu)$ . The compaction of the FGG allows a significant reduction of the macro porosity and hinders this convective flux.

The use of smaller grains (FGG 10/30) or of a wider granulometric range (mix 10/30 and 10/60) is another solution to minimise the bulk porosity and thus the effective thermal conductivity, although the compacted material appears to show the best performance.

The use of another FGG typology (FGG red), which presents a more stable grain structure, provides a slightly better performance in comparison to the uncompact 10/60 configuration, but it is still outperformed by the compacted 10/60.

An important outcome from this investigation is that the installation of the insulating material is as important as its selection. The adoption of loose FGG without an homogeneous compaction, although apparently more performant than the bounded FGG, does not provide an efficient insulation because of the cited additional convective heat transfer within the bulk.

## 8. CONCLUSIONS AND OUTLOOK

The aim of this work was the definition of useful indications for the insulation in large-scale TES systems in terms of both material selection and structural configuration. Thanks to the study of the realised pre-mock-up, FGG appears to be an interesting candidate, due to its structural properties, ease of installation and stability of thermal properties even at high temperatures. Moreover, its cost per unit volume appears to be comparable with the traditional synthetic insulation materials. Under this perspective, FGG filled insulating bore piles can represent a promising solution to help reduce insulation installation costs, since they do not require the use of scaffolding for their installation.

From numerical simulations it appears that the effective performance of the structure with bounded primary piles is lower compared to the one with non-bounded primary piles, although the use of a more dense solution (i.e. lower distance between the piles) guarantees some improvement.

Another important aspect, which emerged from the pre-mock-up, is the convective heat transfer that occurs within the porous FGG piles in case of a high temperature heat sink (i.e. TES). The heat transfer is linked with the temperature difference between the storage and the surroundings; therefore, the necessary degree of compaction or the use of additional convection barriers depends on the temperature level of the TES. Further studies on the influence of the thermal stratification of the water within the TES are ongoing.

Further field test with a real scale mock-up are planned, in order to investigate the structural stability of compacted FGG and its drillability. Within these tests, the feasibility of realising bore piles with homogeneously compressed FGG is also tested. A continuous compaction is ideal for the bulk homogeneity, yet it requires more frequent compaction intervals, longer time and more material. The investigation of the final installation costs considering this additional compression phase are ongoing.

The quality of TES insulation is defined through two main parameters: ground temperature and thermal losses. Ground temperature is an environmental parameter, useful to evaluate the influence of the TES on the surroundings. However, the use of insulation has a further objective to maintain high storage efficiencies. The study of the thermal losses is in this respect an important indicator of the TES efficiency from the system point of view. Investigations on the

thermal performance of the FGG in a humid environment (i.e. ground) are also advisable.

Overall, the adoption of effective thermal insulation in buried TES is an important feature in the construction of TES systems in order to support the integration and expansion of renewable energy sources in DH systems with minimal impact on the surrounding environment.

## AUTHORS' CONTRIBUTIONS

**Alice Tosatto:** Conceptualization, Methodology, Data collection and analysis, Software, Writing – original draft. **Fabian Ochs:** Funding acquisition, Conceptualization, Scientific support, Writing – review & editing. **Abdulrahman Dahash:** Scientific support, Writing – review & editing. **Christoph Muser, Felix Kutscha-Lissberg, Peter Kremnitzer:** Conceptualization, Writing – review & editing.

## ACKNOWLEDGMENTS

This research was carried out under the Austrian flagship research project “Giga-Scale Thermal Energy Storage for Renewable Districts” (giga\_TES, Project Nr.: 860949), financed by the Austrian “Klima- und Energiefonds” and performed in the frame of the program “Energieforschung”. Therefore, the authors wish to acknowledge the financial support for this work.

Additionally, the authors wish to thank Geocell Schaumglas for providing the material used for the experimental set up.

## REFERENCES

- [1] J. O. Dalenbäck, “Ranking List of European Large Scale Solar Heating Plants,” 2017. [Online]. Available: <https://www.solar-district-heating.eu/en/plant-database/>.
- [2] PlanEnergi, “Long term storage and solar district heating A presentation of the Danish pit and borehole thermal energy storages in Brædstrup, Marstal, Dronninglund and Gram,,” 2016. [Online]. Available: <https://planenergi.eu/activities/district-heating/seasonal-heat-storage/>.
- [3] A. Sørensen and T. Schmidt, “Design and Construction of Large Scale Heat Storages for District Heating in Denmark,” in *International Conference on Energy Storage*, 2018, no. April, [Online]. Available: <http://planenergi.dk/wp-content/uploads/2018/05/Soerenen-and->

- Schmidt\_Design-and-Construction-of-Large-Scale-Heat-Storages-12.03.2018-004.pdf.
- [4] A. Dahash, F. Ochs, A. Tosatto, and W. Streicher, "Toward efficient numerical modeling and analysis of large-scale thermal energy storage for renewable district heating," *Appl. Energy*, vol. 279, 2020, doi: 10.1016/j.apenergy.2020.115840.
- [5] F. Ochs, A. Zottl, M. Lauermann, H. Schranzhofer, C. Halmdienst, and D. Reiterer, "Store4Grid: Optimierte Erdbecken-Wärmespeicher für Wärmenetze," 2015.
- [6] A. Dahash, F. Ochs, G. Giuliani, and A. Tosatto, "Understanding the interaction between groundwater and large-scale underground hot-water tanks and pits," *Sustain. Cities Soc.*, vol. 71, p. 102928, Aug. 2021, doi: 10.1016/j.scs.2021.102928.
- [7] F. Ochs, A. Dahash, A. Tosatto, and M. Bianchi Janetti, "Techno-economic planning and construction of cost-effective large-scale hot water thermal energy storage for Renewable District heating systems," *Renew. Energy*, vol. 150, 2020, doi: 10.1016/j.renene.2019.11.017.
- [8] F. Ochs, "Modelling Large-Scale Thermal Energy Stores," University of Stuttgart, 2009.
- [9] *VDI-Wärmeatlas*, 10th ed. Springer Verlag, 2006.
- [10] ÖNORM B 8110-7, "Wärmeschutz im Hochbau - Teil 7: Tabellierte wärmeschutztechnische Bemessungswerte." 2013.
- [11] W. Villasmil, L. J. Fischer, and J. Worlitschek, "A review and evaluation of thermal insulation materials and methods for thermal energy storage systems," *Renewable and Sustainable Energy Reviews*, vol. 103, 2019, doi: 10.1016/j.rser.2018.12.040.
- [12] "GigaTES," *Giga-scale thermal energy storage for renewable districts*, 2021. <https://www.gigates.at/index.php/en/>.
- [13] D. Adam, A. Andreatta, W. Feist, and J. Feix, "Grundlagenforschung Glas-schaumgranulatschüttungen als lastabtragender und wärmedämmender Baustoff - Berichte aus Energie- und Umweltforschung," 2015.
- [14] International Energy Agency (IEA), "SHC Task 45 Large System Seasonal thermal energy storage - Report on state of the art and necessary further R + D," Stuttgart (Germany), 2015. [Online]. Available: [http://task45.iea-shc.org/data/sites/1/publications/IEA\\_SHC\\_Task45\\_B\\_Report.pdf](http://task45.iea-shc.org/data/sites/1/publications/IEA_SHC_Task45_B_Report.pdf).
- [15] M. Bianchi Janetti, T. Plaz, F. Ochs, O. Klesnil, and W. Feist, "Thermal conductivity of foam glass gravels: A comparison between experimental data and numerical results," in *6th Int. Build. Phys. Conf. IBPC 2015, Torino, Italy*, 2015, vol. 78, pp. 3258–3263, doi: 10.1016/j.egypro.2015.11.713.
- [16] F. Ochs, M. Bianchi, and J. Ondrej Klesnil, "Wärmeleitfähigkeit von Schüttungen aus Glasschaumgranulat: Messtechnische Analyse sowie Analytische und Numerische Modellierung," 2015. [Online]. Available: [http://www.aee-now.at/cms/fileadmin/downloads/projekte/store4grid/store4Grid\\_Wärmeleitfähigkeit.pdf](http://www.aee-now.at/cms/fileadmin/downloads/projekte/store4grid/store4Grid_Wärmeleitfähigkeit.pdf).
- [17] F. P. Incropera, D. P. Dewitt, T. L. Bergman, and A. S. Lavine, *Incropera's Principles of Heat and Mass Transfer*, Global Edi. Wiley, 2017.